Ultrasonics Sonochemistry 86 (2022) 106011

Contents lists available at ScienceDirect

Ultrasonics Sonochemistry

journal homepage: www.elsevier.com/locate/ultson

Airborne ultrasonic application on hot air-drying of pork liver. Intensification of moisture transport and impact on protein solubility

E.A. Sánchez-Torres [a], B. Abril [a], J. Benedito [a], J. Bon [a], M. Toldrà [b], D. Parés [b], J.V. García-Pérez [a,*]

[a] UPV, Universitat Politècnica de València. Department of Food Technology. Camí de Vera, s/n, 46022, Valencia, Spain
[b] UdG, University of Girona, Institute of Food and Agricultural Technology (INTEA), XIA (Catalonian Network on Food Innovation), Escola Politècnica Superior, C/ Maria Aurèlia Capmany 61, 17003 Girona, Spain

ARTICLE INFO

Keywords:
Meat by-products
Dehydration
Meat protein
Novel technologies
Airborne ultrasound transmission

ABSTRACT

Nowadays, there is increasing interest in developing strategies for the efficient and sustainable use of animal by-products, such as pork liver. In order to stabilize the product, a prior dehydration stage may be required due to its high perishability. The water removal process of pork liver is energy costly and time consuming, which justifies its intensification using novel technologies. In this sense, the aim of this study was to assess the effect of the airborne application of power ultrasound on the hot air-drying of pork liver. For that purpose, drying experiments were carried out at 30, 40, 50, 60 and 70 °C on pork liver cylinders at 2 $m{\cdot}s^{-1}$ with (US) and without ultrasonic application (AIR). The drying process was modeled from the diffusion theory and, in the dried pork liver, the protein solubility was analyzed in order to determine the effect of drying on the protein quality. The ultrasound application increased the drying rate, shortening the drying time by up to 40% at 30 °C. The effect of power ultrasound at high temperatures (60 and 70 °C) was of lesser magnitude. Drying at 70 °C involved a noticeable reduction in the protein solubility for dried liver, while the impact of ultrasound application on the solubility was not significant ($p > 0.05$).

1. Introduction

Liver is one of the most interesting edible pork by-products from a nutritional point of view since it constitutes a good source of proteins, vitamins A, B_{12}, C and D, and minerals, such as iron, zinc and copper [1]. Despite this, household demand for fresh liver has been progressively declining in the last few decades due to consumer trends and, nowadays, it is of low commercial value. Therefore, the use of pork liver is mainly limited to the manufacturing of liver paste products and animal feed [2] and could be considered a by-product or even a residue in slaughterhouses. Of the different revalorization strategies that are being investigated, those that could be highlighted are aiming to extract its high protein fraction (81.9 %, d.b.) [3] since the liver is considered as a protein source of high biological value and digestibility [4]. In this sense, the functional protein fraction of pork liver has exhibited adequate emulsifying, gelling and foaming properties compared to other commercial proteins widely used in the meat industry [5]. In addition, from its non-functional protein fraction, biopeptides with antioxidant and antimicrobial activity could also be obtained by hydrolysis [6,7]. Furthermore, pork liver contains a high concentration of Ferrochelatase, which is an enzyme that catalyzes the formation of Zinc protoporphyrin IX (ZnPP). ZnPP is a natural red pigment that, due to its stability to light and heat, might be useful as a means of improving the color of meat products, avoiding or minimizing the controversial use of nitrites/nitrates [8–10].

The further use of meat by-products, such as pork liver, other viscera or blood, is complex due to its low biological stability, potential source of pathogenic microorganisms, high water content, rapid auto oxidation and high level of endogenous enzyme activity [11]. In order to overcome these problems, a prior dehydration stage could be used in order to stabilize the product and at the same time reduce its weight and volume. Thus, a reduction in the moisture content might facilitate the further processing of the pork liver in order to obtain its protein fraction and incorporate it into different processed foods. Any research into the drying process should not only encompass strategies linked to highly efficient processes in terms of the drying rate, energy consumption and investment cost but also investigate how drying affects the product quality. In the particular case of pork liver, a sustainable drying process should also consider its impact on the protein fraction quality and

* Corresponding author.
E-mail address: jogarpe4@tal.upv.es (J.V. García-Pérez).

https://doi.org/10.1016/j.ultsonch.2022.106011
Received 20 January 2022; Received in revised form 22 March 2022; Accepted 16 April 2022
Available online 22 April 2022

Nomenclature

Bi_m	Mass transfer Biot number, dimensionless
d.b.	Dry basis
D_0	Pre-exponential factor of Arrhenius equation for D_e, $m^2 \cdot s^{-1}$
D_e	Effective moisture diffusivity, $m^2 \cdot s^{-1}$
E_a	Activation energy, $kJ \cdot mol^{-1}$
k	Mass transfer coefficient, $kg \cdot m^{-2} \cdot s^{-1}$
k_0	Pre-exponential factor of Arrhenius equation for k, $kg \cdot m^2 \cdot s^{-1}$
L	Sample half-thickness, m
L_c	Characteristic length, m
M	Number of model parameters
MRE	Mean relative error, %
N	Number of experimental data
PS	Protein solubility, g soluble protein·(g total protein)$^{-1}$, %
R	Sample radius, m
$\overline{R}$	Universal gas constant, $kJ \cdot mol^{-1} \cdot K^{-1}$
r	Radial direction, m
S_y	Standard deviation of the sample, kg water·(kg dry solid)$^{-1}$
S_{yx}	Standard deviation of the estimation, kg water·(kg dry solid)$^{-1}$
T	Drying air temperature, K
t	Drying time, s
TP	Total protein, g total protein·(g dried liver)$^{-1}$, %, d.b.
VAR	Explained variance, %
W	Moisture content of sample, kg water·(kg dry solid)$^{-1}$
W_0	Initial moisture content of sample, kg water·(kg dry solid)$^{-1}$
W_p	Local moisture content, kg water·(kg dry solid)$^{-1}$
W_e	Equilibrium moisture content, kg water·(kg dry solid)$^{-1}$
$W_{i\ calc}$	Estimated moisture content i, kg water·(kg dry solid)$^{-1}$
$W_{i\ exp}$	Experimental moisture content i, kg water·(kg dry solid)$^{-1}$
$\overline{W_{exp}}$	Average of experimental moisture values, kg water·(kg dry solid)$^{-1}$
z	Axial direction, m
α	Eigenvalues
φ_{air}	Relative humidity of drying air
φ_e	Equilibrium relative humidity with surface moisture of solid
ψ	Dimensionless moisture
ρ_{ds}	Dry solid density, $kg \cdot m^{-3}$
ρ_w	Water density, $kg \cdot m^{-3}$

functionality. In this sense, a preliminary analysis of protein solubility in the dried material could be useful as a means of assessing the impact on the quality of the drying process [12]. Protein solubility is usually the first functional property determined during the development and testing of new protein ingredients. Protein solubility is a physicochemical property that is related to other functional properties, and knowing this can provide useful information on the potential utilization of proteins and their functionality, especially in foams, emulsions and gels [13].

Of the different existing dehydration methods, convective hot air-drying has been used worldwide for centuries to preserve food and agricultural products. The convective drying of foods is a combined heat and mass transfer operation and can be performed using natural convection or forced-air. The modeling and optimization of convective drying require an understanding of the transport mechanisms inside and between the solid matrix and the drying air, as well as knowledge of the thermal, equilibrium and transport properties of both systems [14,15]. Water removal during drying is jointly modulated by both internal and external resistances to mass transfer. The internal resistance encompasses the movement of water within the solid matrix and so it is an inherent property of the foodstuff but can be affected by drying conditions, such as air temperature. The external resistance controls the water transfer from the solid surface to the drying air and depends on the thickness of the convective boundary layer [16]. In order to simplify the modeling of the drying process, external resistance is sometimes neglected, especially when high air-flow rates are used [17]. Therefore, mechanistic drying modelling of a particular food commodity has to evaluate the relevance of both transport phenomena.

The application of air-borne ultrasound represents a feasible alternative means of accelerating the mass transfer process during the convective drying of foodstuffs, since it can influence both internal and external resistances based on non-thermal mechanisms [18,19]. On the one hand, ultrasonic waves produce a rapid series of alternate contractions and expansions (sponge effect) of the solid matrix in which they are traveling. This alternating stress improves the internal diffusion of water molecules and additionally, could generate microscopic channels that make the moisture transport easier. In addition, high-intensity acoustic waves could potentially cause the cavitation of water molecules inside the food material, which can be beneficial for the removal of the tightly bound moisture [20]. On the other hand, airborne ultrasound introduces pressure variations, oscillating velocities and micro-streaming at solid/fluid interfaces, and, hence, increases the external transport rate of moisture [21,22]. Thus, ultrasound-assisted convection drying allows the use of lower temperatures to maintain drying rates and, hence, has been proven useful for the drying of heat-sensitive materials, such as fruits and vegetables [23–25]. However, air-borne ultrasound application and its development present some practical difficulties, which should be addressed if it is implemented industrially. Since air is a highly attenuating medium that absorbs the acoustic energy, the main difficulty of the application of ultrasound is the transmission of the acoustic wave from the surface of the transducer to the samples. Furthermore, the high impedance difference between the air and the solid involves the reflection of a high proportion of the applied acoustic energy, preventing the acoustic energy transfer to the solids being treated [26,27]. Therefore, research into the mechanisms of ultrasonic wave transmission in gas–solid media and the improvement of current transducers for further industrial implementation is a matter of relevant research [28].

Despite the current interest in the development of strategies for an effective and sustainable use of edible meat by-products [29–32], no references to the drying of pork liver or of other edible offal have been found. Moreover, the performance of ultrasound application in drying processes is largely dependent on the structure of the food material and, therefore, must be evaluated when analyzing new matrices [18], since the extrapolation of results obtained from other matrices is complex and inaccurate. Hence, the aim of this study was to assess the influence of the air temperature and the application of air-borne ultrasound on the hot air convective drying of pork liver. For that purpose, experimental drying kinetics were carried out and modeled using the diffusion theory and the protein solubility of dried pork liver was analyzed in order to determine the effect of drying on the protein quality.

2. Materials and methods

2.1. Raw material and sample preparation

Fresh pork livers were purchased from a local market (Valencia, Spain), transported at a temperature of under 4 °C and processed in <2 h. The fresh livers were divided into four portions according to their main lobes, vacuum packaged (EV-13, Tecnotrip, Barcelona, Spain), frozen in a blast chiller (RDM051S, Hiber, Veneto, Italy) and stored at −20 °C until processing. Approximately two hours before the drying

experiments, the liver pieces were partially thawed at 4 °C in order to obtain cylindrical samples (12.6 mm in diameter and 15 mm in height) using a household tool.

2.2. Air-drying experiments

The drying of the pork liver samples was carried out in a pilot-scale convective dryer (Fig. 1). The drying chamber (1, Fig. 1A) is the primary element of this equipment and it consists of an aluminum vibrating cylinder (internal diameter 100 mm, height 310 mm and thickness 10 mm) driven by a piezoelectric ultrasonic transducer (21.8 kHz) (2, Fig. 1A) generating a high-intensity ultrasonic field inside the chamber. The temperature and air flow were controlled using a PID control algorithm. The weight of the samples was automatically recorded at regular time intervals (5 min) during drying and the relative humidity and temperature of the room air was also measured. The pork liver cylinders were placed in a sample holder (Fig. 1B) inside the vibrating cylinder.

The experimental design consists of two sets of drying experiments: (i) with (US) and (ii) without ultrasound application (AIR). In the experiments in which ultrasound was applied, an electrical power of 50 W was supplied to the transducer. For both sets, an air velocity of 2 $m{\cdot}s^{-1}$ was used at five different temperatures: 30, 40, 50, 60 and 70 °C. Three replicates were carried out for each drying condition. The sample used in each experiment consisted of 16 cylinders, which presented an average initial weight of 30 ± 1 g. The experiments were extended until reaching a weight loss of 60% with a weighing interval of 5 min. In all the experiments, the initial and final moisture contents were determined gravimetrically by dehydration at 105 °C until constant weight (24 h), following the AOAC 950.46B method [33].

2.3. Mathematical modeling

A diffusion model based on Fick's 2nd law was used to describe the moisture content evolution in the drying of pork liver cylinders. The differential equation of diffusion was formulated combining Fick's law and a differential mass balance. Thus, for isotropic solids and finite cylindrical geometry the resulting equation (Eq. (1)) is as follows:

$$\frac{\partial W_p(r,z,t)}{\partial t} = D_e\left(\frac{\partial^2 W_p(r,z,t)}{\partial r^2} + \frac{\partial^2 W_p(r,z,t)}{\partial z^2} + \frac{1}{r}\frac{\partial W_p(r,z,t)}{\partial r}\right) \quad (1)$$

where r and z are the characteristic directions (radial and axial, respectively) of the water transport in the cylindrical geometry. The same effective moisture diffusivity (D_e) was considered for each characteristic direction considering the liver as a material without a typical structural pattern and its value was assumed to be constant in all the moisture ranges considered. Effective moisture diffusivity is the kinetic parameter of Eq. (1), which entails not only the molecular diffusion phenomena but also other unknown effects influencing the internal transport, such as the phenomena linked to the ultrasound application [34].

In order to solve Eq. (1), initial and boundary conditions are needed. Some of the assumptions considered are common for the models tested in this paper: (i) the initial moisture content and temperature are uniform inside the sample, (ii) the drying process is isothermal considering that the possible thermal effect of the ultrasound application is negligible compared to a high vibrating effect, and (iii) the shape and volume of the solid remains constant during the drying period considered. Starting from these assumptions, two kinds of models of differing complexities have been proposed: (i) the NER model assumes the process is entirely controlled by internal diffusion neglecting any interference of the air flow, and (ii) the ER model assumes a joint control of diffusion and convective transport.

2.3.1. Model neglecting external resistance (NER)

If the external resistance to mass transfer is negligible, the internal resistance controls the process. Therefore, the diffusion of the internally adsorbed water in the solid matrix is the rate-limiting factor of the drying process. This aspect is included in the model through the boundary conditions considering the solid surface enters equilibrium with the air instantaneously (Eqs. (2) and (3)).

$$t > 0 \quad r = R; \quad 0 \le r \le R \quad W_p(R,z,t) = W_e \quad (2)$$

$$t > 0 \quad z = L; \quad 0 \le z \le L \quad W_p(r,L,t) = W_e \quad (3)$$

The analytical solution of the governing equation (Eq. (1)) considering these boundary conditions should be integrated for the entire volume of the cylinder so as to obtain the average moisture content of the samples ($W(t)$). This solution considers the finite cylinder geometry (2L height and R radius) as the intersection of an infinite slab (thickness equal to 2L) and an infinite cylinder (radius equal to R) and is given by Eq. (4):

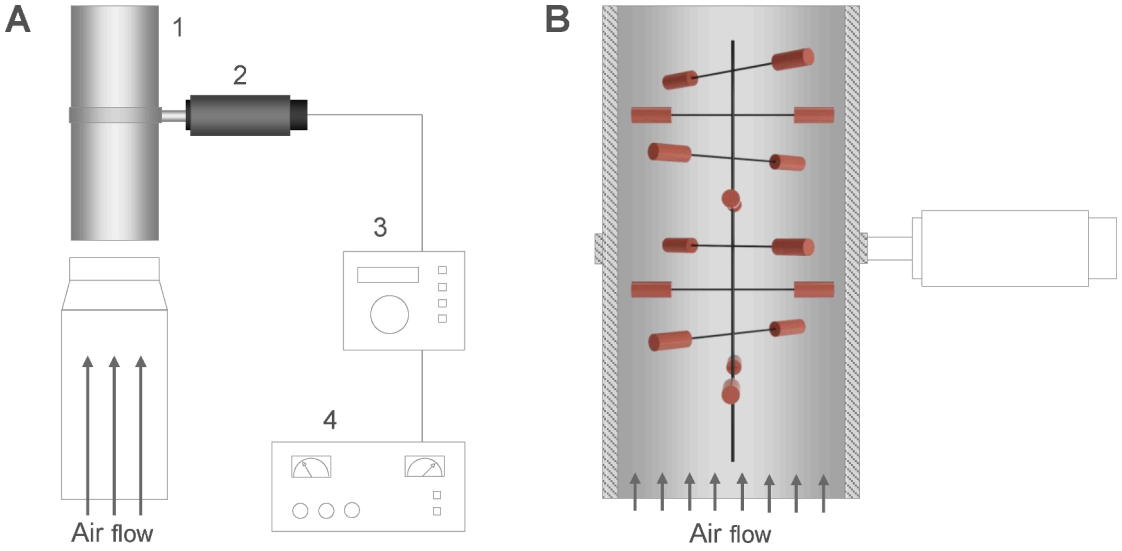

Fig. 1. A. Experimental set-up for convective ultrasound-assisted drying: 1. Vibrating cylinder – Drying chamber, 2. Ultrasound transducer, 3. Impedance electronic controller, 4. Ultrasonic power generator. B. Detail of the sample holder inside the drying chamber and the arrangement of liver cylinders.

$$\psi(t) = \left[\sum_{n=0}^{\infty} \frac{8}{(2n+1)^2\pi^2} \exp\left(-\frac{D_e(2n+1)^2\pi^2 t}{4L^2}\right)\right] \times \left[\sum_{n=1}^{\infty} \frac{4}{{\alpha_n}^2} \exp\left(-\frac{D_e {\alpha_n}^2 t}{R^2}\right)\right] \quad (4)$$

where $\psi(t)$ is the dimensionless moisture as a function of the drying time and is defined by Eq. (5):

$$\psi(t) = \frac{W(t) - W_e}{W_0 - W_e} \quad (5)$$

The α represent the eigenvalues and are the roots of the Bessel function of the first kind of order zero. The equilibrium moisture contents (W_e) were obtained from the previously reported desorption data of pork liver [35]. Thus, the effective moisture diffusivity (D_e) was considered as the model parameter, and its value was identified using an optimization procedure minimizing the sum of the squared differences between the experimental and the calculated average moisture contents of the samples. For that purpose, the Generalized Reduced Gradient (GRG) optimization method, available in the Microsoft Excel spreadsheet (Microsoft Office 2019, Microsoft Corp., Redmond, WA, USA), was used.

2.3.2. Model considering external resistance (ER)

When considering the external resistance to mass transfer to be noticeable compared to the internal, the boundary conditions shown in Eqs. (2) and (3) should be replaced by Eqs. (6) and (7), respectively. This new assumption considers that the water flow that reaches the solid matrix surface by diffusion is transferred to the surrounding air by convection.

$$t > 0 \quad r = R; \quad 0 \le r \le R$$
$$-D_e\rho_{ds}\frac{\partial W_p(R,z,t)}{\partial r} = k(\varphi_e(R,z,t) - \varphi_{air}) \cdot \quad (6)$$

$$t > 0 \quad z = L; \quad 0 \le z \le L$$
$$-D_e\rho_{ds}\frac{\partial W_p(r,L,t)}{\partial z} = k(\varphi_e(r,L,t) - \varphi_{air}) \quad (7)$$

where k is the mass transfer coefficient computing the rate of water transfer from the solid surface to the air flow [36]. Thus, k is a kinetic parameter computing not only convection but also other phenomena influencing external transport, such as the already mentioned effects of ultrasound on the solid-air interface.

If the diffusion model (Eq. (1)) assumes boundary conditions reflected in Eqs. (6) and (7), it is not possible to find an analytical solution for the governing equation, and it is necessary to use a numerical method. In this paper, the model was solved using the finite element method, which reduces the problem defined in the geometric space, in order to find a solution at a finite number of points by subdividing the domain into smaller regions, forming a mesh of "elements". Unlike finite difference procedures, the governing equation in the finite element method is integrated over each finite element, and the contributions added up ("assembled") throughout the problem domain. Thus, a set of finite linear equations is obtained in terms of the values of the unknown parameters at the element nodes. The solutions to these equations are achieved using linear algebra procedures [37]. In order to solve the diffusion model described by applying the finite element method, the COMSOL Multiphysics software (v. 3.4, COMSOL Inc., Burlington, MA, USA) was used. Subsequently, a non-linear optimization procedure was applied to jointly identify the values of the effective moisture diffusivity (D_e) and the mass transfer coefficient (k), which were set as the model parameters in this case. For that purpose, the *surrogateopt* function from the MATLAB (v. R2019b, The MathWorks Inc., Natick, MA, USA) scripting environment was used, which is suitable for the global minimization of time-consuming objective functions. The objective function chosen was also the sum of the squared differences between the experimental and calculated average moisture contents.

2.3.3. Evaluation of the diffusion models

The goodness-of-fit of the proposed diffusion models to the experimental drying kinetics was evaluated by computing the mean relative error (MRE) (Eq. (8)) and the explained variance (VAR) (Eq. (9)).

$$\mathrm{MRE} = \frac{100}{N}\sum_{i=1}^{N}\frac{|W_{i\ exp} - W_{i\ calc}|}{W_{i\ exp}} \quad (8)$$

$$\mathrm{VAR} = \left(1 - \frac{S_{yx}^2}{S_y^2}\right)100 \quad (9)$$

The standard deviation of the sample (S_y) and the standard deviation of the estimation (S_{yx}) are defined by the following expressions:

$$S_y = \sqrt{\frac{1}{N-1}\sum_{i=1}^{N}\left(W_{i\ exp} - \overline{W_{exp}}\right)^2} \quad (10)$$

$$S_{yx} = \sqrt{\frac{1}{N-M}\sum_{i=1}^{N}\left(W_{i\ exp} - W_{i\ calc}\right)^2} \quad (11)$$

The MRE indicates the relative error of the predictions and it is a criterion used to assess the fit of a model to experimental data. Values of MRE below 10% reflect reasonably good mathematical descriptions for most practical purposes. The VAR represents the relative variance explained by the model with respect to the total variance, and it varies from 0 to 100%.

2.4. Influence of temperature on kinetic parameters

The effect of temperature on the effective moisture diffusivity (D_e) or moisture transfer coefficient (k) can be described by an Arrhenius type relationship (Eqs. (12) and (13), respectively) [14,38].

$$D_e = D_0 \ \exp\left(-\frac{E_a}{\overline{R}T}\right) \quad (12)$$

$$k = k_0 \ \exp\left(-\frac{E_a}{\overline{R}T}\right) \quad (13)$$

Therefore, by means of the linearization of Eqs. (12) and (13), the activation energy of the drying process (E_a) was calculated from the plot of the natural logarithms of D_e or k vs T^{-1}, respectively. The activation energy identified according to each kinetic parameter was compared between both experimental sets considered (AIR and US).

2.5. Mass transfer Biot number

The ratio of internal to external resistance to mass transfer was computed from the Biot number (Bi_m) [39] using Eq. (14) with the parameters identified by means of the ER model (D_e and k).

$$Bi_m = \frac{kL_c}{\rho_w D_e} \quad (14)$$

where the radius of the cylinder (R) was considered as the characteristic length (L_c). The density of the fluid (ρ_w), in this case water, was set for each drying temperature at atmospheric pressure.

2.6. Protein solubility

The protein solubility of dried pork liver samples was analyzed by means of the method described by Morr et al. [40] with slight

modifications. In order to ensure negligible residual moisture content in the dried material, the dried liver cylinders were ground and vacuum-dried at 30 °C for 24 h and vacuum packaged (EV-13, Tecnotrip, Barcelona, Spain) until analyzed. Afterwards, 1 g of ground dried liver samples was diluted in distilled water (100 mL). The liver solutions were stirred for 30 min on a magnetic stirring plate, avoiding vortex formation. After stirring, aliquots of the solutions were centrifuged at 20,000 × g for 30 min at 20 °C (Sorvall RC-SC plus, DuPont Co., Newtown, CT, USA) and decanted. Protein solubility was calculated as the percentage of soluble protein content in the supernatant in relation to the total protein content in the dried liver sample, both protein contents being determined by the Kjeldahl method AOAC 954.01 [33]. Each determination was performed in duplicate for each replicate and drying condition. It is worth mentioning that in the present study the use of raw liver was not considered to obtain the protein solubility due to its high perishability.

2.7. Statistical analysis

In order to assess the influence of the air temperature and the application of power ultrasound on both the drying kinetic parameters (effective moisture diffusivity and mass transfer coefficient), as well as on the total protein and the protein solubility of the dried liver samples, a multifactor ANOVA was carried out, and the means compared by computing the LSD (Least Significance Difference) intervals. Furthermore, a hypothesis test was computed on the comparison of the slopes of the regression linear models in order to determine significant differences between the activation energies of the two experimental sets (AIR and US). The confidence interval for the estimated activation energy was identified from the confidence interval of the slope of the regression model [41]. A 95 % confidence level was used in every case. The statistical analysis was performed by means of R programming language (v. 4.0.3) [42].

3. Results and discussion

3.1. Experimental drying data

Fig. 2 shows the experimental drying kinetics of pork liver cylinders at different temperatures with (US) and without (AIR) ultrasound application. From the beginning, drying occurred at falling-rate, reflecting the relevance of diffusion internal transport as the primary controlling mechanism of water removal. Hence, the initial average moisture content (2.71 ± 0.01 d.b.) was considered as the critical one. In Fig. 2, the drying kinetics are plotted until reaching a moisture content of 0.5 d.b., which represents a weight loss of 60 %, approximately. As expected, as the temperature increased, the drying rate was higher in both experimental sets (AIR and US). For this reason, in order to reach an average moisture content of 0.5 d.b. in the AIR experiments, 22 h were necessary at 30 °C, while the drying process was completed in only 4 h at 70 °C. At low temperatures, the ultrasound application also increased the drying rate, as can be observed if the AIR and US experiments at 30 °C are compared (Fig. 2). Thus, the drying time necessary to reach an average moisture content of 0.5 d.b. was 22 h for AIR experiments at 30 °C, while it was only 13 h for US experiments. This reflects a shortening of the drying time of approximately 40%, which is consistent with the reduction reported for other protein-rich matrices, such as cod, using the same airborne ultrasonic set-up and under similar experimental conditions [43]. To our knowledge, no previous references exist to the use of airborne-assisted ultrasonic drying of animal muscles or organs, such as liver or heart. For beef and chicken meat slabs, Başlar et al. [44] found a similar shortening of the drying time using direct-contact ultrasound-assisted vacuum drying. Higher percentages of drying time reduction (60–80 %) have been reported when airborne ultrasound has been applied in the drying of fruits and vegetables, which is likely to be related to the structure of the food material [45]. In this

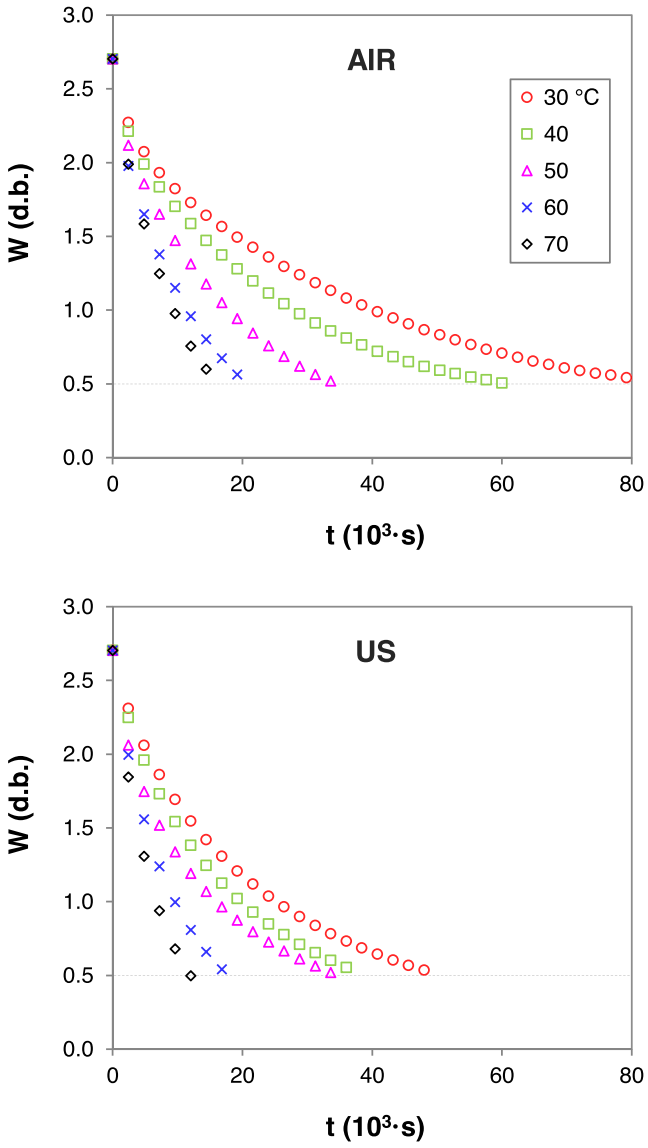

Fig. 2. Experimental drying kinetics of pork liver without (AIR) and with ultrasound application (US) at 30, 40, 50, 60 and 70 °C.

sense, Ozuna et al. [18] determined that soft and porous structures exhibit a lower acoustic impedance and, therefore, a better coupling with the air than hard and dense products, which involves a very different response to airborne ultrasound-assisted drying.

As can be observed in Fig. 2, as the temperature increased, the influence of ultrasound decreased, almost disappearing at temperatures above 50 °C. Similar behavior has been previously reported in the airborne ultrasound-assisted drying of other products such as carrot [46] and apple [47,48]. This could be explained by assuming that ultrasound waves transfer a certain amount of energy into the solid, thus improving the water mobility. Nevertheless, as temperature rises, the water mobility linked to the thermal energy increases and the relative influence of the acoustic energy on the water mobility is minimized [49].

3.2. NER diffusion model

In order to quantify the influence of temperature and power ultrasound application on the drying rate of pork liver, the model described by Eq. (4) was fitted to the experimental drying kinetics (Table 1). Specifically, the effective moisture diffusivity identified ($\times 10^{-11}$ $m^2 \cdot s^{-1}$) for AIR experiments ranged from 9.86 at 30 °C to 31.13 at 70 °C; in the

Table 1
Effective moisture diffusivity (D_e) identified from the model that neglects the external resistance (NER) for AIR and US experiments and statistical parameters: average explained variance (VAR) and mean relative error (MRE).

T (°C)	AIR			US		
	$D_e \times 10^{11}$ ($m^2 \cdot s^{-1}$)	VAR (%)	MRE (%)	$D_e \times 10^{11}$ ($m^2 \cdot s^{-1}$)	VAR (%)	MRE (%)
30	9.86 ± 0.80^{a}	98.70	5.25	13.23 ± 1.63^{ab}	96.73	8.52
40	13.73 ± 0.55^{ab}	97.80	7.00	19.40 ± 1.60^{abc}	96.13	9.68
50	18.53 ± 1.45^{abc}	96.30	9.11	22.73 ± 2.56^{bcd}	98.67	5.18
60	27.30 ± 1.95^{cd}	95.90	10.22	31.70 ± 10.31^{de}	96.83	8.11
70	31.13 ± 1.90^{de}	93.20	12.87	37.70 ± 13.83^{e}	95.43	9.57

Average of $D_e \pm$ standard deviation ($N = 3$). Superscripts a, b, c, d and e show homogeneous groups established from LSD (least significant difference) intervals ($p < 0.05$).

case of the US experiments, meanwhile, effective moisture diffusivity ranged from 13.23 to 37.70 at 30 and 70 °C, respectively. Hence, as can be observed in Table 1, the higher the drying air temperature, the greater the effective moisture diffusivity for both kinds of experiments. In addition, the ultrasound application increased the effective moisture diffusivity at all the experimental temperatures tested. Thus, from a multifactorial ANOVA, both temperature and ultrasound were found to have a significant influence ($p < 0.05$) on the effective diffusivity. The computed effective diffusivities fall within the range identified by previous studies for the drying of other protein matrices such as beef [50–52], pork [53,54] or chicken [55,56].

The influence of air temperature on the effective diffusivity identified by the NER model for AIR and US experiments followed an Arrhenius type relationship, as Fig. 3A illustrates. According to the hypothesis test on the comparison of the slopes of the regression lines, no significant differences were found ($p > 0.05$) between either experimental set for the estimated activation energy. Therefore, values of 25.89 ± 5.38 and 22.41 ± 4.80 kJ·mol^{-1} were obtained for the AIR and US set, respectively. In such a way, the energy needed for water removal was not affected by ultrasound application. The activation energy figures (kJ·mol^{-1}) are close to those proposed by other authors for meat and fish products under similar drying conditions: marinated beef, 28.21 [50], raw pork, 25.94 [53], raw chicken, 27.85 [56], salted cod, 20.46 [43] or salted shark, 21.94 [57]. Moreover, from Fig. 3A, the effective diffusivity values are easily compared. Thus, it can be observed that the effective diffusivities for the US experiments at 30, 40 and 60 °C were close to the figures identified in the AIR set at 40, 50 and 70 °C, respectively. This suggests that the increase in effective diffusivity produced by ultrasound application could be equivalent to a temperature rise of 10 °C; at least for temperatures below 50 °C, according to the experimental drying kinetics found (Fig. 2). This increase found in the effective diffusivity might also be related to the possible thermal effect of the ultrasound application, which has been previously reported in some products [58]. In this sense, despite the ultrasound application is widely considered as a non-thermal technology in food processing [59,60], some studies have reported a noticeable effect of ultrasound application on the temperature rise during drying in both the air flow [19] and the product [61]. However, other authors catalogued the thermal effect of ultrasound as low compared to a high vibrating effect [62]. In addition, literature has reported that airborne application may improve both internal heat conduction and external convection [63,64], which makes complicated to ascribe the featured thermal effect to a heat generation due to wave absorption or the improvement of heat transport. Further studies should carefully evaluate the thermal effect in the particular case of pork liver within well-controlled experimental conditions.

The ability of the NER model for the mathematical description was evaluated by computing the explained variance (VAR) and the mean relative error (MRE) (Table 1). For the AIR experiments the VAR ranged from 98.71 (30 °C) to 93.24 % (70 °C) and the MRE from 5.25 (30 °C) to 12.87 % (70 °C). Hence, the NER model lost the ability to describe the drying kinetics as the temperature rose in the AIR set. This could be linked to the fact that the importance of external convective transport on controlling drying rate grows as the temperature rises. Therefore, in AIR experiments, the temperature rise resulted in a larger increase on the internal transport compared to the external one. In the case of the US experiments, no temperature-related trend was identified in either VAR or MRE; however, the VAR was around 96% and the MRE close to 10% at the different temperatures tested, which represents an unsatisfactory fit of the NER model when ultrasound is applied. Thus, ultrasound application probably affected the internal resistance to mass transfer, increasing the importance, as controlling mechanism, of external convective transport during the dehydration of the solid matrix. Therefore, the use of a more complex model that includes the external resistance (ER model) seems to be necessary. The application of an ER

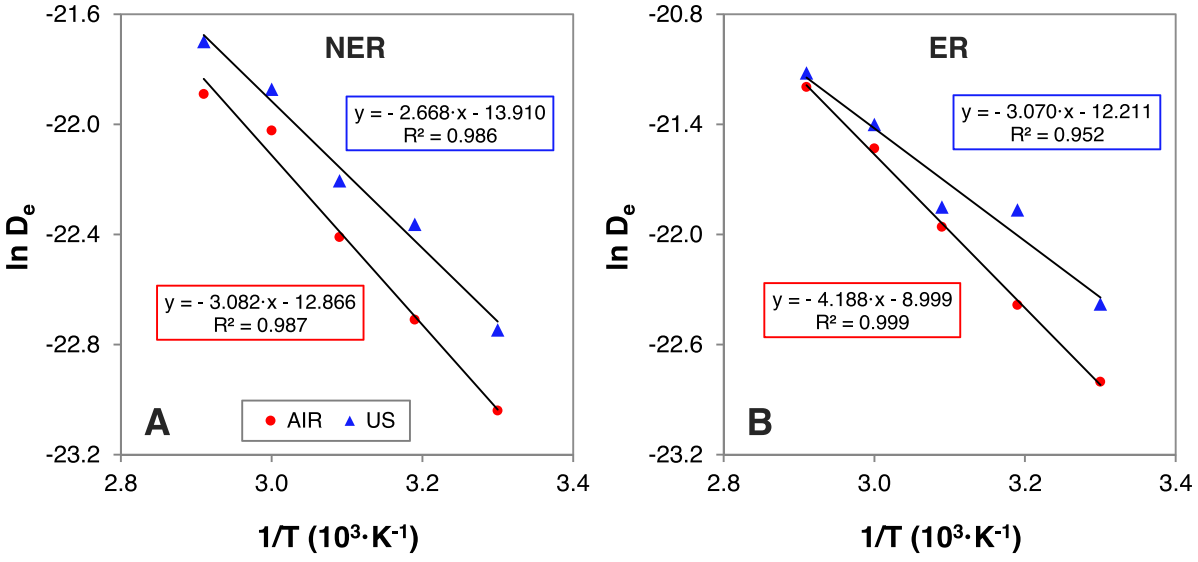

Fig. 3. Influence of air temperature on the average effective moisture diffusivities (D_e) identified by means of the NER (A) and ER (B) models.

model would have two goals; firstly, to obtain a satisfactory fit of the experimental drying data, and secondly, to contribute to an analysis of the influence of ultrasound application on the internal and external resistance to mass transfer from the analysis of the identified parameters (D_e and k).

3.3. ER diffusion model

Experimental drying data were also analyzed by fitting the ER model, which considers the external resistance to mass transfer, jointly identifying the effective moisture diffusivity (D_e) and the external mass transfer coefficient (k) (Table 2). Thus, for both types of experiments (AIR and US), the explained variance (VAR) was around 98 % in every case with a mean relative error (MRE) of below 10%, which indicates an adequate fit to the experimental data. Therefore, the introduction of the external resistance in the model contributed to a better mathematical description, as can also be observed in Fig. 4, in which the performance of the ER and NER models are compared for a particular case (AIR at 70 °C). For the purposes of enhancing the model's fitting ability, further studies should analyze other relevant aspects, such as the sample shrinkage or heat transport, in order to improve the mechanistic modelling and identify more reliable figures for the kinetic parameters. Furthermore, the ultrasound application involves different physical phenomena that depend on the interaction of the ultrasonic wave with the matter. Hence, modeling the wave transmission through the air and the solid matrix might be of interest in order to assess the overall effect of the airborne ultrasound application. In this sense, Kowalski et al. [65] addressed this issue from a mechanistic model based on coupled heat, mass and momentum transfer equations, which considered the propagation of ultrasonic wave in the air and through a saturated porous material. Nevertheless, this study neglected the high energy loss by reflection on the product interface, a key behavior as described by Ozuna et al. [18]. In addition, experimental validation of complex mechanistic models results excessively complicated and, therefore, may be discouraged depending on the purpose of the study [34].

As can be observed in Table 2, between 30 and 70 °C, the effective diffusivity ($\times 10^{-11}$ $m^2 \cdot s^{-1}$) ranged from 12.50 to 62.31 for the AIR set and from 19.12 to 67.22 for the US set, these figures being slightly higher than those identified for the NER model. The mass transfer coefficient ($\times 10^{-5}$ $kg \cdot m^{-2} \cdot s^{-1}$) ranged from 8.36 to 16.50 for the AIR set and from 10.83 to 23.05 for the US set, at 30 and 70 °C respectively. These values are close to the mass transfer coefficients identified for other products, such as persimmons [17] or apples [47] under similar drying conditions. Thus, as the air-drying temperature rose, the effective moisture diffusivity and the mass transfer coefficient increased for both AIR and US experimental sets. Moreover, the ultrasound application caused a reduction in the internal and external resistance to mass transfer, as a result of the increase found in both the effective moisture diffusivity and the mass transfer coefficient, respectively, at the different experimental temperatures (Table 2). Hence, both temperature and ultrasound significantly ($p < 0.05$) affected the effective diffusivity and the mass transfer coefficient.

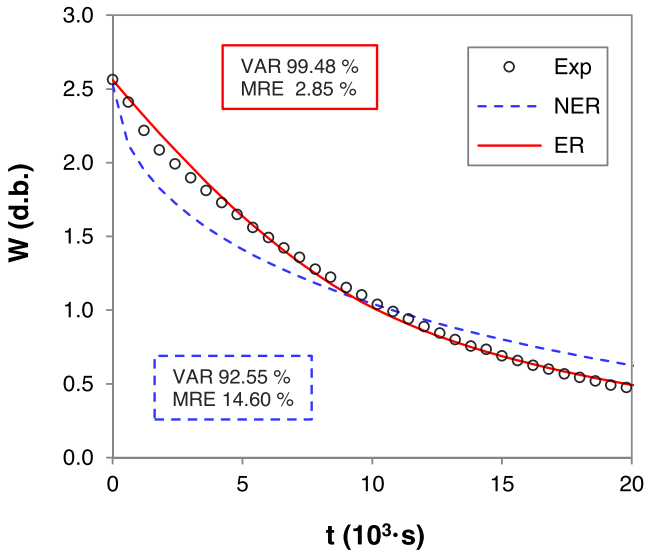

Fig. 4. Experimental drying kinetics and kinetics calculated using the NER and ER diffusion models for an AIR experiment at 70 °C.

The effective diffusivity identified by the ER model also followed an Arrhenius type relationship with the temperature in both experimental sets, as can be seen in Fig. 3B. Unlike the results found with the NER model, there was a significant ($p < 0.05$) difference between the estimated activation energy of the AIR and US sets, according to the hypothesis test on the comparison of the slopes of the regression lines. Thus, activation energy figures of 35.18 ± 2.41 and 25.72 ± 10.49 $kJ \cdot mol^{-1}$ were computed for the AIR and US experiments, respectively. In this sense, it seems that the application of ultrasound reduced the energy required to remove the water from the solid matrix. Furthermore, Fig. 3B reflects that the estimated effective diffusivities at 30 and 40 °C for the US set were similar to the figures identified at 40 and 50 °C for the AIR set, respectively. While, the effective diffusivities corresponding to the temperatures of 50, 60 and 70 °C were very similar in both experimental sets. Therefore, it seems to be confirmed again that ultrasound application takes a primary role at drying temperatures below 50 °C and, from this threshold on, its effect is reduced. In this regard, García-Pérez et al. [46] found similar behavior when analyzing the convective drying of carrots (30–70 °C, 1 $m \cdot s^{-1}$); ultrasound application increased the drying rate at the different temperatures tested, but the improvement in the drying rate lessened at high temperatures, and almost disappeared at 70 °C.

Fig. 5 shows that the estimated mass transfer coefficient also followed an Arrhenius type relationship with the temperature in both experimental sets. The activation energy was not significantly affected

Table 2
Effective moisture diffusivity (D_e) and moisture transfer coefficient (k) estimated using the model that considers the external resistance (ER) for AIR and US experiments and statistical parameters: average explained variance (VAR) and mean relative error (MRE).

T (°C)	AIR				US			
	$D_e \times 10^{11}$ ($m^2 \cdot s^{-1}$)	$k \times 10^5$ ($kg \cdot m^{-2} \cdot s^{-1}$)	VAR (%)	MRE (%)	$D_e \times 10^{11}$ ($m^2 \cdot s^{-1}$)	$k \times 10^5$ ($kg \cdot m^{-2} \cdot s^{-1}$)	VAR (%)	MRE (%)
30	12.50 ± 1.25^{a}	8.36 ± 0.83^{u}	98.19	6.08	19.12 ± 1.19^{ab}	10.83 ± 3.42^{uv}	97.77	6.45
40	19.01 ± 1.54^{ab}	9.31 ± 0.82^{uv}	97.98	6.05	31.88 ± 5.10^{abc}	12.14 ± 0.78^{vw}	98.39	4.89
50	29.05 ± 0.75^{abc}	10.85 ± 1.17^{uv}	98.64	4.91	32.43 ± 2.97^{abc}	16.35 ± 0.56^{xy}	97.86	6.65
60	44.59 ± 1.45^{bcd}	14.75 ± 1.96^{wx}	98.24	5.66	50.81 ± 23.05^{cd}	18.59 ± 1.90^{y}	98.51	5.56
70	62.31 ± 1.07^{d}	16.50 ± 2.63^{xy}	99.01	3.64	67.22 ± 40.74^{d}	23.05 ± 2.39^{z}	98.33	5.21

Average of D_e and k ± standard deviation ($N = 3$). Superscripts a, b, c, d, and u, v, w, x, y, z, show homogeneous groups established from LSD (least significant difference) intervals ($p < 0.05$) for effective diffusivity and moisture transfer coefficient, respectively.

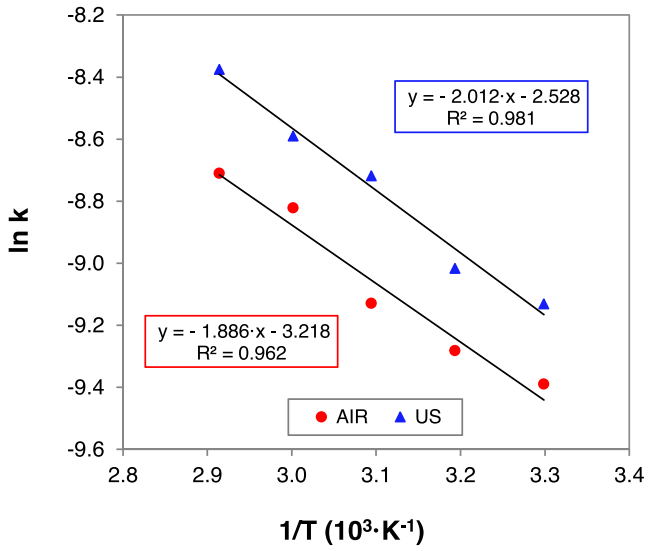

Fig. 5. Influence of air temperature on the average moisture transfer coefficients (k) identified by means of the ER model.

($p > 0.05$) by ultrasound application; thus, the figures reported were 15.68 ± 6.02 and 16.73 ± 4.33 kJ·mol^{-1} for the AIR and US sets, respectively. Fig. 5 illustrates that the increase found in the mass transfer coefficient brought about by ultrasound application could be equivalent to a temperature rise of between 10 and 20 °C.

The mass transfer Biot number allowed computing the relationship between the internal and external resistance for each drying experiment. In the AIR set, the Biot number ranged from 4.23 ± 0.14 to 1.71 ± 0.27, at 30 and 70 °C, respectively (Fig. 6). Thus, as the temperature increased, the Biot number approached the unit and, hence, the difference between the internal and external resistance decreased, probably as a consequence of a larger increase on the internal transport compared to the external one. This fact is consistent with the decreasing trend of the explained variance (VAR) observed in the NER model for the AIR set (Fig. 6; Table 1), which again illustrates that the diffusion control is more relevant at low temperatures. In the US set, no clear trend of Biot number with temperature was found, ranging from 4.01 ± 1.37 to 2.47 ± 0.50. This may indicate that the ultrasound application affects similarly the internal and external resistance to mass transfer. Both the drying temperature and the use of ultrasound could affect the quality

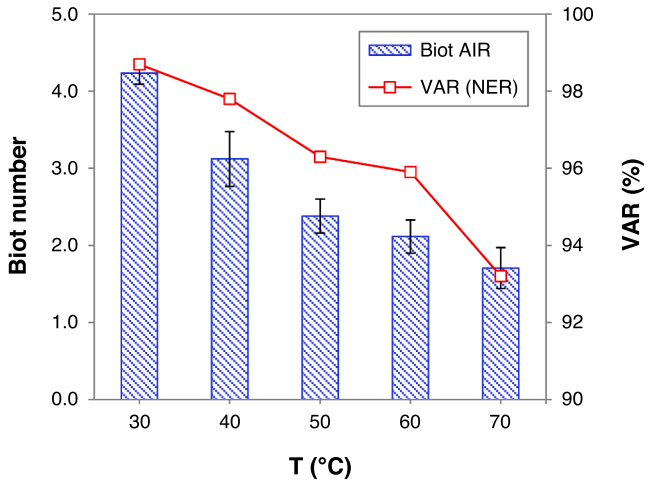

Fig. 6. Influence of air temperature on the average mass transfer Biot number computed from the ER model parameters (D_e and k) and explained variance (VAR) of the NER model in the AIR set.

characteristics of the liver protein, of which solubility is of the greatest importance for industrial applications.

3.4. Protein solubility

In order to assess the protein quality of pork liver after the drying process, the protein solubility in water was analyzed. High solubility is generally a requisite for successful functional applications of protein ingredients in foods. Protein solubility (PS) was calculated as the percentage of soluble protein content relative to the total protein content (TP) for dried liver obtained under different drying conditions (Table 3).

Total protein contents in the dried liver ranged from 64.73 ± 2.12 to 70.54 ± 3.11 % in AIR experiments and from 63.30 ± 3.36 to 67.85 ± 3.63 % in US. Thus, as expected, neither temperature nor ultrasound application were significant factors ($p > 0.05$) in the percentage of total protein in the dried liver. The figures obtained are close to the total protein range found in the literature for pork liver (in dry basis), 68.5–78.3 % [66], although drastically lower values have also been reported, 50.4 % [67]. Differences in the reported protein contents could be ascribed to the protein/fat ratio (the two main components in addition to water), which is conditioned by differences in nutritional factors, physiological state, sex, genetic background and age [68].

The protein solubility ranged from 25.86 ± 1.97 to 46.93 ± 7.51 % and from 25.20 ± 9.01 to 40.45 ± 4.02 % for AIR and US sets, respectively. As observed in Table 3, the drying temperature significantly ($p < 0.05$) influenced the protein solubility, while the application of ultrasound did not represent a significant impact ($p > 0.05$). Drying at 70 °C led to a marked reduction in the protein solubility, resulting in an average drop of 36.53 % compared to samples dried at 30 and 40 °C, with and without ultrasound application. In contrast, the protein solubility remained fairly constant for liver dried at temperatures between 30 and 60 °C, obtaining an average value of 38.78 ± 4.51 % considering jointly the AIR and US sets at this temperature range. The protein solubility in the dried liver reflects a large difference compared to the protein solubility in water previously reported for fresh pork liver: 76.1 % [69] and 78.6 % [5]. On the one hand, this could be explained by conformational changes in the structure of the protein that result in an alteration of protein solubility, caused by the joint effect of thermal protein denaturation and water removal during drying. This has already been evidenced in the heating of different muscle matrices [13]. On the other hand, Nuckles et al. [69] and Steen et al. [5] extracted the water soluble protein with phosphate buffer instead of the distilled water used in this study. In all likelihood, the phosphate buffer helps to extract a larger quantity of proteins compared to those extracted by the distilled water. In this sense, analyzing raw turkey and buffalo liver and using distilled water as the extracting medium, Zouari et al. [70] and Devatkal et al. [71] found percentages of protein solubility of 55 and 20–40% respectively, which was closer to the figures obtained in the present

Table 3
Protein solubility (PS) and total protein (TP) for pork liver dried without (AIR) and with (US) ultrasound application at 30, 40, 50, 60 and 70 °C.

T (°C)	AIR		US	
	PS (%)	TP (%, d.b.)	PS (%)	TP (%, d.b.)
30	35.98 ± 4.43^{bc}	69.71 ± 3.54^{xy}	37.53 ± 2.54^{abc}	67.39 ± 1.80^{xyz}
40	46.93 ± 7.51^{a}	65.66 ± 5.35^{xyz}	40.45 ± 4.02^{ab}	67.03 ± 3.40^{xyz}
50	40.41 ± 4.94^{ab}	70.54 ± 3.11^{x}	37.38 ± 0.69^{abc}	63.51 ± 6.18^{yz}
60	41.88 ± 9.82^{ab}	64.73 ± 2.12^{yz}	29.66 ± 2.10 ^{cd}	63.30 ± 3.36^{yz}
70	25.86 ± 1.97^{d}	69.81 ± 3.22^{xy}	25.20 ± 9.01^{d}	67.85 ± 3.63^{xyz}

Average percentage of protein solubility (PS) and total protein (TP) for dried liver ± standard deviation ($N = 3$). Superscripts a, b, c, d, and x, y, z, show homogeneous groups established from LSD (least significant difference) intervals ($p < 0.05$) for the percentage of protein solubility (PS) and total protein (TP), respectively.

study. Similar results were reported in protein concentrates from goose liver at pH 6–7 [4]. Moreover, the difference between the soluble protein contents in the present analysis and the studies by Nuckles et al. [69] and Steen et al. [5] for pork liver might also be attributed to the aforementioned aspects, such as nutritional factors, the physiological state, sex, genetic background or age. These particular differences would also explain the wide experimental variability found in the present study. Furthermore, it has been found that the application of ultrasound during liver drying did not significantly affect ($p > 0.05$) the protein solubility. This could reflect that the ultrasonic waves did not alter the structure of the pork liver protein. In contrast, it is widely accepted that the use of high-intensity ultrasound can induce structural changes in the protein molecules [72–74]. However, this has been reported for protein solutions using an ultrasound probe or bath, which implies an acoustic energy transfer into the liquid solution, which is several orders of magnitude higher than the use of air-borne ultrasound applied in the present study. Moreover, the conformational changes associated with the drying process might have masked those produced by ultrasound application.

4. Conclusions

The application of high-intensity ultrasound during the hot air-drying of pork liver increased the drying rate, shortening the drying time by up to 40% at 30 °C. As the temperature rose, the influence of ultrasound decreased, almost disappearing at temperatures above 50 °C. The reduction in the drying time when ultrasound was applied was also evidenced by the increase in both the effective moisture diffusivity and the convection mass transfer coefficient at low temperatures. The protein solubility remained fairly constant for liver dried from 30 to 60 °C, while drying at 70 °C led to a large reduction in the soluble protein fraction. Further studies should analyze how the drying process affects other thermolabile compounds in pork liver, which could justify the application of ultrasound in low-temperature drying from both productivity and energy points of view. In addition, the thermal effect of the airborne ultrasound application on drying should be carefully addressed in order to determine if a noticeable temperature increase exists in both air and product, which would contribute to explain, at least partially, the increase in the drying rate when ultrasound is applied.

CRediT authorship contribution statement

E.A. Sánchez-Torres: Software, Formal analysis, Writing – original draft. **B. Abril:** Investigation, Formal analysis, Writing – original draft. **J. Benedito:** Conceptualization, Writing – review & editing. **J. Bon:** Formal analysis, Conceptualization, Supervision, Validation, Writing – review & editing. **M. Toldrà:** Investigation, Validation, Writing – review & editing. **D. Parés:** Methodology, Validation, Writing – review & editing. **J.V. García-Pérez:** Conceptualization, Supervision, Methodology, Writing – review & editing.

Declaration of Competing Interest

The authors declare that they have no known competing financial interests or personal relationships that could have appeared to influence the work reported in this paper.

Acknowledgements

The authors acknowledge the financial support from the “Ministerio de Economía y Competitividad (MINECO)” and “Instituto Nacional de Investigación y Tecnología Agraria y Alimentaria (INIA)” in Spain (Project RTA2017-00024-C04-03). Eduardo A. Sanchez-Torres acknowledges the FPU PhD contract (FPU18/01439) granted by the Spanish Ministry of Science, Innovation and Universities. Funding for open access charge: Universitat Politècnica de València.

References

[1] Ockerman HW, Basu L, Toldrá F. Chapter 22 - Edible By-products. In: Toldrá FBT-LMS (Eighth E, editor. Woodhead Publ. Ser. Food Sci. Technol. Nutr., Woodhead Publishing; 2017, p. 679–96. https://doi.org/https://doi.org/10.1016/B978-0-08-100694-8.00022-4.
[2] F. Toldrá, L. Mora, M. Reig, New insights into meat by-product utilization, Meat Sci. 120 (2016) 54–59, https://doi.org/10.1016/j.meatsci.2016.04.021.
[3] M. Babicz, K. Kropiwiec-Domańska, M. Szyndler-Nędza, A.M. Grzebalska, I. Łuszczewska-Sierakowska, A. Wawrzyniak, et al., Physicochemical parameters of selected internal organs of fattening pigs and wild boars, Ann. Anim. Sci. 18 (2018) 575–591.
[4] X. Li, S. Xue, X. Zhao, X. Zhuang, M. Han, X. Xu, G. Zhou, Gelation properties of goose liver protein recovered by isoelectric solubilisation/precipitation process, Int. J. Food Sci. Technol. 53 (2) (2018) 356–364.
[5] L. Steen, S. Glorieux, O. Goemaere, K. Brijs, H. Paelinck, I. Foubert, I. Fraeye, Functional properties of pork liver protein fractions, Food Bioprocess Technol. 9 (6) (2016) 970–980.
[6] T. Lafarga, M. Hayes, Bioactive peptides from meat muscle and by-products: generation, functionality and application as functional ingredients, Meat Sci. 98 (2014) 227–239, https://doi.org/10.1016/j.meatsci.2014.05.036.
[7] L. Mora, M. Reig, F. Toldrá, Bioactive peptides generated from meat industry by-products, Food Res. Int. 65 (2014) 344–349, https://doi.org/10.1016/j.foodres.2014.09.014.
[8] H. De Maere, S. Chollet, E. Claeys, C. Michiels, M. Govaert, E. De Mey, H. Paelinck, I. Fraeye, In vitro zinc protoporphyrin IX formation in different meat sources related to potentially important intrinsic parameters, Food Bioprocess Technol. 10 (1) (2017) 131–142.
[9] J.-I. Wakamatsu, N. Murakami, T. Nishimura, A comparative study of zinc protoporphyrin IX-forming properties of animal by-products as sources for improving the color of meat products, Anim Sci J 86 (5) (2015) 547–552.
[10] B. Abril, E.A. Sanchez-Torres, R. Bou, J.V. Garcia-Perez, J. Benedito, Ultrasound intensification of Ferrochelatase extraction from pork liver as a strategy to improve ZINC-protoporphyrin formation, Ultrason. Sonochem. 78 (2021) 105703, https://doi.org/10.1016/j.ultsonch.2021.105703.
[11] K. Jayathilakan, K. Sultana, K. Radhakrishna, A.S. Bawa, Utilization of byproducts and waste materials from meat, poultry and fish processing industries: a review, J. Food Sci. Technol. 49 (3) (2012) 278–293, https://doi.org/10.1007/s13197-011-0290-7.
[12] R. Căpriță, A. Căpriță, I. Crețescu, Protein solubility as quality index for processed soybean, Sci Pap Anim Sci Biotechnol 43 (2010) 375–378.
[13] J.F. Zayas, Functionality of Proteins in Food, Springer, Berlin Heidelberg, 2012.
[14] C. Ratti, Advances in Food Dehydration, CRC Press, 2008.
[15] V.S. Eim, D. Urrea, C. Rosselló, J.V. García-Pérez, A. Femenia, S. Simal, Optimization of the drying process of carrot (Daucus carota v. Nantes) on the basis of quality criteria, Dry Technol 31 (8) (2013) 951–962, https://doi.org/10.1080/07373937.2012.707162.
[16] Mulet A, Cárcel JA, Sanjuan N, García-Pérez J V. Food dehydration under forced convection conditions. 2010:153–77.
[17] J.A. Cárcel, J.V. García-Pérez, E. Riera, A. Mulet, Influence of high-intensity ultrasound on drying kinetics of persimmon, Dry Technol. 25 (1) (2007) 185–193.
[18] C. Ozuna, T. Gómez Álvarez-Arenas, E. Riera, J.A. Cárcel, J.V. Garcia-Perez, Influence of material structure on air-borne ultrasonic application in drying, Ultrason. Sonochem. 21 (2014) 1235–1243, https://doi.org/10.1016/j.ultsonch.2013.12.015.
[19] J.V. Garcia-Perez, J.A. Carcel, S. Simal, M.A. García-Alvarado, A. Mulet, Ultrasonic intensification of grape stalk convective drying: kinetic and energy efficiency, Dry Technol. 31 (8) (2013) 942–950, https://doi.org/10.1080/07373937.2012.716128.
[20] H.T. Sabarez, J.A. Gallego-Juarez, E. Riera, Ultrasonic-assisted convective drying of apple slices, Dry Technol. 30 (9) (2012) 989–997, https://doi.org/10.1080/07373937.2012.677083.
[21] J.A. Cárcel, J.V. García-Pérez, J. Benedito, A. Mulet, Food process innovation through new technologies: Use of ultrasound, J. Food Eng. 110 (2012) 200–207, https://doi.org/10.1016/j.jfoodeng.2011.05.038.
[22] J.V. Santacatalina, J.R. Soriano, J.A. Cárcel, J.V. Garcia-Perez, Influence of air velocity and temperature on ultrasonically assisted low temperature drying of eggplant, Food Bioprod. Process. 100 (2016) 282–291, https://doi.org/10.1016/j.fbp.2016.07.010.
[23] Ó. Rodríguez, V. Eim, C. Rosselló, A. Femenia, J.A. Cárcel, S. Simal, Application of power ultrasound on the convective drying of fruits and vegetables: effects on quality, J. Sci. Food Agric. 98 (5) (2018) 1660–1673, https://doi.org/10.1002/jsfa.2018.98.issue-510.1002/jsfa.8673.
[24] F.A.N. Fernandes, S. Rodrigues, J.V. García-Pérez, J.A. Cárcel, Effects of ultrasound-assisted air-drying on vitamins and carotenoids of cherry tomatoes, Dry Technol. 34 (8) (2016) 986–996, https://doi.org/10.1080/07373937.2015.1090445.
[25] J. Gamboa-Santos, A. Montilla, A.C. Soria, J.A. Cárcel, J.V. García-Pérez, M. Villamiel, Impact of power ultrasound on chemical and physicochemical quality indicators of strawberries dried by convection, Food Chem. 161 (2014) 40–46, https://doi.org/10.1016/j.foodchem.2014.03.106.
[26] K. Fan, M. Zhang, A.S. Mujumdar, Application of airborne ultrasound in the convective drying of fruits and vegetables: A review, Ultrason. Sonochem. 39 (2017) 47–57, https://doi.org/10.1016/j.ultsonch.2017.04.001.

[27] J.V. García-Pérez, J.A. Cárcel, J. Benedito, A. Mulet, Power ultrasound mass transfer enhancement in food drying, Food Bioprod. Process 85 (2007) 247–254, https://doi.org/10.1205/fbp07010.
[28] R.R. Andrés, E. Riera, J.A. Gallego-Juárez, A. Mulet, J.V. García-Pérez, J.A. Cárcel, Airborne power ultrasound for drying process intensification at low temperatures: Use of a stepped-grooved plate transducer, Dry Technol. 39 (2) (2021) 245–258, https://doi.org/10.1080/07373937.2019.1677704.
[29] S.Y. Lee, S.Y. Yoon, D.Y. Lee, O.Y. Kim, H.S. Kim, E.Y. Jung, K.C. Koh, S.J. Hur, Development of batch processing to obtain bioactive materials from pork byproducts, Anim. Prod. Sci. 60 (2) (2020) 316, https://doi.org/10.1071/AN18600.
[30] M.I. Sarwar, M.S. Hussain, A.R. Leghari, Heparin can be isolated and purified from bovine intestine by different techniques, Int. J. Pharm. Sci. Invent. 2 (2013) 21–25.
[31] S.Y. Yoon, O.Y.K. Da Young Lee, S.Y. Lee, S.J. Hur, Development of commercially viable method of conjugated linoleic acid synthesis using linoleic acid fraction obtained from pork by-products, Korean J. Food Sci. Anim. Resour. 38 (2018) 693.
[32] E. Álvarez-Castillo, C. Bengoechea, A. Guerrero, Composites from by-products of the food industry for the development of superabsorbent biomaterials, Food Bioprod. Process. 119 (2020) 296–305, https://doi.org/10.1016/j.fbp.2019.11.009.
[33] AOAC, Official Methods of Analysis of AOAC International, 21st ed., AOAC International, Gaithersburg, Maryland, 2019.
[34] Villamiel M, Riera E, García-Pérez JV. The use of ultrasound for drying, degassing and defoaming of foods 2021.
[35] E.A. Sánchez-Torres, B. Abril, J. Benedito, J. Bon, J.V. García-Pérez, Water desorption isotherms of pork liver and thermodynamic properties, LWT 149 (2021), 111857, https://doi.org/10.1016/j.lwt.2021.111857.
[36] G.D. Saravacos, Z.B. Maroulis, Transport Properties Of Foods, CRC Press, 2001.
[37] D.W. Pepper, J.C. Heinrich, The Finite Element Method: Basic Concepts and Applications with MATLAB, MAPLE, and COMSOL, third ed., CRC Press, 2017.
[38] N. Sanjuán, M. Lozano, P. García-Pascual, A. Mulet, Dehydration kinetics of red pepper (Capsicum annuum L var Jaranda), J. Sci. Food Agric. 83 (2003) 697–701, https://doi.org/10.1002/jsfa.1334.
[39] M. Parti, Mass transfer Biot numbers, Period Polytech Mech Eng 38 (1994) 109–122.
[40] C.V. Morr, B. German, J.E. Kinsella, J.M. Regenstein, J.P.V.A.N. Buren, A. Kilara, et al., A collaborative study to develop a standardized food protein solubility procedure, J. Food Sci. 50 (1985) 1715–1718, https://doi.org/10.1111/j.1365-2621.1985.tb10572.x.
[41] J.J. Faraway, Linear Models with R, CRC Press, 2014.
[42] R Core Team. R: A Language and Environment for Statistical Computing 2021.
[43] C. Ozuna, J.A. Cárcel, P.M. Walde, J.V. Garcia-Perez, Low-temperature drying of salted cod (Gadus morhua) assisted by high power ultrasound: Kinetics and physical properties, Innov. Food Sci. Emerg. Technol. 23 (2014) 146–155, https://doi.org/10.1016/j.ifset.2014.03.008.
[44] M. Başlar, M. Kılıçlı, O.S. Toker, O. Sağdıç, M. Arici, Ultrasonic vacuum drying technique as a novel process for shortening the drying period for beef and chicken meats, Innov. Food Sci. Emerg. Technol. 26 (2014) 182–190, https://doi.org/10.1016/j.ifset.2014.06.008.
[45] J.A. Gallego-Juarez, K.F. Graff, Power Ultrasonics: Applications of High-Intensity Ultrasound, Elsevier Science, 2018.
[46] García-Pérez J V, Rosselló C, Cárcel JA, De la Fuente S, Mulet A. Effect of air temperature on convective drying assisted by high power ultrasound. Defect Diffus. forum, vol. 258, Trans Tech Publ; 2006, p. 563–74.
[47] Ó. Rodríguez, J.V. Santacatalina, S. Simal, J.V. Garcia-Perez, A. Femenia, C. Rosselló, Influence of power ultrasound application on drying kinetics of apple and its antioxidant and microstructural properties, J. Food Eng. 129 (2014) 21–29, https://doi.org/10.1016/j.jfoodeng.2014.01.001.
[48] F.A.N. Fernandes, S. Rodrigues, J.A. Cárcel, J.V. García-Pérez, Ultrasound-assisted air-drying of apple (Malus domestica L.) and its effects on the vitamin of the dried product, Food Bioprocess Technol. 8 (7) (2015) 1503–1511, https://doi.org/10.1007/s11947-015-1519-7.
[49] Mulet A, Cárcel J, Garcia-Perez J V, Riera E. Ultrasound-Assisted Hot Air Drying of Foods, 2010, p. 511–34. https://doi.org/10.1007/978-1-4419-7472-3_19.
[50] F.C. Muga, T.S. Workneh, M.O. Marenya, Modelling the thin-layer drying of beef biltong processed using hot air drying, J. Biosyst. Eng. 45 (4) (2020) 362–373, https://doi.org/10.1007/s42853-020-00076-5.
[51] M. Chabbouh, A. Sahli, S. Bellagha, Does the spicing step affect the quality and drying behaviour of traditional kaddid, a Tunisian cured meat? J. Sci. Food Agric. 93 (14) (2013) 3634–3641, https://doi.org/10.1002/jsfa.6319.
[52] E. Akello Mewa, M. Wandayi Okoth, C. Nkirote Kunyanga, M. Njue Rugiri, Drying modelling, moisture diffusivity and sensory quality of thin layer dried beef, Curr. Res. Nutr. Food Sci. J. 6 (2) (2018) 552–565.
[53] P. Gou, J. Comaposada, J. Arnau, Moisture diffusivity in the lean tissue of dry-cured ham at different process times, Meat Sci. 67 (2004) 203–209, https://doi.org/10.1016/j.meatsci.2003.10.007.
[54] G. Clemente, J. Bon, N. Sanjuán, A. Mulet, Drying modelling of defrosted pork meat under forced convection conditions, Meat Sci. 88 (3) (2011) 374–378.
[55] C.L. Hii, C.E. Itam, S.P. Ong, Convective air drying of raw and cooked chicken meats, Dry Technol. 32 (11) (2014) 1304–1309, https://doi.org/10.1080/07373937.2014.924133.
[56] O. Ismail, An experimental and modeling investigation on drying of chicken meat in convective dryer, Stud. Univ. Babes-Bol. Chem. 62 (2017) 459–469.
[57] K.J. Park, Diffusional model with and without shrinkage during salted fish muscle drying, Dry Technol. 16 (3-5) (1998) 889–905, https://doi.org/10.1080/07373939808917443.
[58] M. Bantle, J. Hanssler, Ultrasonic convective drying kinetics of clipfish during the initial drying period, Dry Techno.l 31 (11) (2013) 1307–1316, https://doi.org/10.1080/07373937.2013.792093.
[59] H.Q. Zhang, G.V. Barbosa-Cánovas, V.M.B. Balasubramaniam, C.P. Dunne, D. F. Farkas, J.T.C. Yuan, Nonthermal Processing Technologies for Food, Wiley, 2011.
[60] H.B. Jadhav, U.S. Annapure, R.R. Deshmukh, Non-thermal Technologies for Food Processing, Front Nutr 8 (2021), 657090, https://doi.org/10.3389/fnut.2021.657090.
[61] D. Colucci, D. Fissore, C. Rossello, J.A. Carcel, On the effect of ultrasound-assisted atmospheric freeze-drying on the antioxidant properties of eggplant, Food Res. Int. 106 (2018) 580–588, https://doi.org/10.1016/j.foodres.2018.01.022.
[62] S.J. Kowalski, D. Mierzwa, M. Stasiak, Ultrasound-assisted convective drying of apples at different process conditions, Dry Technol 35 (8) (2017) 939–947, https://doi.org/10.1080/07373937.2016.1239631.
[63] M. Contreras, J. Benedito, J. Bon, J.V. Garcia-Perez, Accelerated mild heating of dry-cured ham by applying power ultrasound in a liquid medium, Innov. Food Sci. Emerg. Technol. 50 (2018) 94–101, https://doi.org/10.1016/j.ifset.2018.10.010.
[64] M. Contreras, J. Benedito, J. Bon, J.V. Garcia-Perez, Intensification of heat transfer during mild thermal treatment of dry-cured ham by using airborne ultrasound, Ultrason. Sonochem. 41 (2018) 206–212, https://doi.org/10.1016/j.ultsonch.2017.09.019.
[65] S.J. Kowalski, A. Rybicki, Ultrasound in wet biological materials subjected to drying, J. Food Eng. 212 (2017) 271–282, https://doi.org/10.1016/j.jfoodeng.2017.05.032.
[66] L.M.L. Nollet, F. Toldrá, Handbook of Analysis Of Edible Animal By-Products, CRC Press, 2011.
[67] M. Estévez, D. Morcuende, R. Ramírez, J. Ventanas, R. Cava, Extensively reared Iberian pigs versus intensively reared white pigs for the manufacture of liver pâté, Meat Sci. 67 (3) (2004) 453–461.
[68] A.J. Clawson, J.D. Garlich, M.T. Coffey, W.G. Pond, Nutritional, physiological, genetic, sex, and age effects on fat-free dry matter composition of the body in avian, fish, and mammalian species: a review, J. Anim. Sci. 69 (1991) 3617–3644, https://doi.org/10.2527/1991.6993617x.
[69] R.O. Nuckles, D.M. Smith, R.A. Merkel, Meat By-product protein composition and functional properties in model systems, J. Food Sci. 55 (1990) 640–643, https://doi.org/10.1111/j.1365-2621.1990.tb05196.x.
[70] N. Zouari, N. Fakhfakh, Amara-Dali W. Ben, M. Sellami, L. Msaddak, M.A. Ayadi, Turkey liver: Physicochemical characteristics and functional properties of protein fractions, Food Bioprod Process 89 (2011) 142–148, https://doi.org/10.1016/j.fbp.2010.03.014.
[71] S. Devatkal, S.K. Mendiratta, N. Kondaiah, M.C. Sharma, A.S.R. Anjaneyulu, Physicochemical, functional and microbiological quality of buffalo liver, Meat Sci. 68 (2004) 79–86, https://doi.org/10.1016/j.meatsci.2004.02.006.
[72] S. Ma, X.u. Yang, C. Zhao, M. Guo, Ultrasound-induced changes in structural and physicochemical properties of β-lactoglobulin, Food Sci. Nutr. 6 (4) (2018) 1053–1064, https://doi.org/10.1002/fsn3.2018.6.issue-410.1002/fsn3.646.
[73] X. Shen, S. Shao, M. Guo, Ultrasound-induced changes in physical and functional properties of whey proteins, Int. J. Food Sci. Technol. 52 (2017) 381–388, https://doi.org/10.1111/ijfs.13292.
[74] H. Hu, J. Wu, E.C.Y. Li-Chan, L.e. Zhu, F. Zhang, X. Xu, G. Fan, L. Wang, X. Huang, S. Pan, Effects of ultrasound on structural and physical properties of soy protein isolate (SPI) dispersions, Food Hydrocoll. 30 (2) (2013) 647–655.